Clays and Clay Minerals, Vol. 51, No. 4, 397–402, 2003.

Cd-SUBSTITUTED GOETHITES – A STRUCTURAL INVESTIGATION BY SYNCHROTRON X-RAY DIFFRACTION

TRANG HUYNH[1,2], ANDREW R. TONG[3], BALWANT SINGH[2,*] AND BRENDAN J. KENNEDY[3]

[1] University of Agriculture and Forestry, Ho Chi Minh City, Vietnam
[2] Faculty of Agriculture, Food and Natural Resources, The University of Sydney, Sydney, NSW 2006, Australia
[3] Centre for Heavy Metal Research, School of Chemistry, The University of Sydney, Sydney, NSW 2006, Australia

Abstract—The structural and physical effects of partially substituting Cd for Fe in goethite have been investigated. The solubility of Cd^{2+} in goethite is ~10 mol.%, *i.e.* $Fe_{0.905}Cd_{0.095}OOH$. The structures of the substituted goethites have been refined, using the Rietveld method, from synchrotron X-ray powder diffraction data. There is a progressive increase in the size of the unit-cell parameters and unit-cell volume, upon the incorporation of much larger Cd^{2+} ion (0.95 Å) compared with Fe^{3+} (0.645 Å) in the goethite structure, together with a reduction in crystallinity. Transmission electron microscopy measurements confirm the crystallite size decreases as the Cd^{2+} content increases in goethite structure.

Key Words—Cadmium, Cd Substitution, Fe Oxides, Goethite, Rietveld Refinement, Synchrotron X-ray Diffraction.

INTRODUCTION

Since the chemical state of soils is highly variable, continual precipitation and dissolution of minerals results in the substitution of mineral components by available cations and anions. In the case of goethite (α-FeOOH), which is the most stable Fe oxide at ambient temperatures, numerous isovalent or heterovalent cations can partially substitute for Fe^{3+}, *e.g.* Ni^{2+}, Zn^{2+}, Cu^{2+}, Cd^{2+}, Al^{3+}, Ga^{3+}, V^{3+}, Mn^{3+}, Co^{3+}, Sc^{3+}, Pb^{4+}, Ge^{4+}, Si^{4+} and Ti^{4+} without a change in the crystal structure (Cornell and Giovanoli, 1988; Cornell and Schwertmann, 1996; Gerth, 1990; Lim-Nunez and Gilkes, 1987; Schwertmann *et al.*, 1989; Singh and Gilkes, 1992). Among these elements Al^{3+} is the most widely studied and has been shown to replace up to 33 mol.% of the Fe in goethite (Cornell and Schwertmann, 1996; Schulze, 1984; Schwertmann and Carlson, 1994). Conversely, there has been only limited research on the degree of substitution of Cd^{2+} in goethite (Gerth, 1990).

Increasing amounts of Cd are being added to soils from several sources, including sewage sludge, fertilizer applications, and mining and smelting operations. At low concentrations the mobility of Cd in soils is controlled by the adsorption-desorption processes, but at higher concentrations, in contaminated environments such as acid mine drainage, Cd^{2+} may coprecipitate with Fe^{3+} in Fe oxides (Singh, 2001). This paper investigates the substitution of Fe^{3+} by Cd^{2+} in goethite and the associated structural perturbations by synchrotron X-ray diffraction (XRD). Further characterization of the compounds was undertaken by laboratory XRD, chemical analysis, Fourier transform infrared (FTIR) spectroscopy, thermogravimetric analysis (TGA), and transmission electron microscopy (TEM).

* E-mail address of corresponding author:
b.singh@acss.usyd.edu.au
DOI: 10.1346/CCMN.2003.0510405

SYNTHESIS

A series of Cd-substituted goethites (nominal mol.% between 0 and 15) of the type $Fe_{1-x}Cd_xOOH$ was prepared by mixing 250 mL of 1 M $Fe(NO_3)_3$ and predetermined volumes of 1 M $Cd(NO_3)_2$ solution with 600 mL of 5 M KOH (Schulze, 1982; Lim-Nunez and Gilkes, 1987). Deionized water was added to make up the volume to 4 L and the pH adjusted to ~13 with KOH. The solutions were aged at ambient temperature (~25ºC) for 16 days, with mixing each day by end-over-end inversion. After ageing, the yellow-brown precipitates were collected by centrifugation and washed five times with 400 mL of deionized water to remove any salts. The electrical conductivity of the final supernatant liquid was approximately equal to that of deionized water. Finally the precipitates were washed with 50 mL of acetone and then dried at 40ºC for 48 h.

In order to remove non-incorporated metals and/or amorphous materials from the goethite samples, five sequential treatments with ammonium oxalate (pH = 3) were undertaken in the dark (Schwertmann, 1964) using a sample to solution ratio of 1:100. The residues were washed thoroughly in deionized water to remove salts and again dried with acetone before further analysis.

INSTRUMENTATION

Total Fe and Cd contents were determined by dissolving the oxalate-treated goethites in concentrated HCl and measuring the metal concentrations with a Varian FT220s flame atomic absorption spectrometer.

Table 1. Total Fe and Cd contents in goethite samples before and after the oxalate treatment as determined by chemical analysis.

Nominal Cd (mol.%)	Before oxalate treatment (mmol/g)		After oxalate treatment (mmol/g)		Actual Cd (mol.%)	x in $Fe_{1-x}Cd_xOOH$
	Cd	Fe	Cd	Fe		
0	0.0	10.422	0.0	10.025	0.00	0
1	0.109	10.560	0.094	9.368	0.99	0.01
2	0.195	9.746	0.165	8.944	1.81	0.02
3	0.292	8.398	0.274	8.738	3.04	0.03
4	0.366	8.737	0.369	8.391	4.21	0.04
5	0.365	6.793	0.454	8.498	5.07	0.05
6	0.495	8.725	0.465	8.580	5.14	0.052
8	0.687	8.436	0.554	8.887	5.87	0.06
10	0.772	7.963	0.883	8.076	9.86	0.1

Conventional laboratory XRD patterns were recorded using a Siemens D5000 diffractometer over the 2θ range 15–75º, in 0.01º steps using a CuKα radiation (λ = 1.5418 Å).

The synchrotron powder XRD patterns were recorded at a wavelength of 0.94779 Å in 0.01º intervals on the Debye-Scherrer diffractometer at the Australian National Beamline Facility (ANBF) Beamline 20B at the Photon Factory (KEK), Tsukuba, Japan. Two image plates covering angular ranges 5–45º and 45–85º were used as detectors. The finely ground samples were placed in glass capillaries (0.3 mm diameter) that were rotated during the collection of XRD patterns. The data were not corrected for absorption and this, presumably, is the origin of the negative atomic displacement parameter observed for O1 in the structural refinements.

Transmission electron microscopy (TEM) studies were performed on a Philips Biofilter microscope fitted with a LaB_6 filament and a lithium-drifted silicon detector, and operated at 120 kV. Samples were prepared by air drying a drop of very dilute suspension on a carbon-coated copper grid. Between 34 and 56 single crystals were examined for each sample, and the area (calculated by summing all of the contiguous pixels in the image), length (longest chord connecting any two points on the perimeter of the feature), and breadth (minimum caliper diameter determined every 11.25º) were measured.

The FTIR spectra were collected using a Bio-Rad FTS-40 spectrophotometer fitted with a drift accessory. Powdered samples were prepared using a KBr matrix: goethite ratio of 4:1.

Thermogravimetric analyses were performed using a TA Instrument TGA 2950. Samples of ~20 mg were heated in Pt crucibles from ambient to 400ºC using a heating rate of 10ºC/min and under a N_2 atmosphere, flowing at ~40–50 mL/min.

RESULTS AND DISCUSSION

Laboratory XRD patterns showed that the only crystalline phase present in the samples containing up to 10 mol.% Cd was the desired goethite phase. The detection limit of the diffractometer is ~2 wt.%. The diffraction patterns of samples containing >10 mol.% Cd contained mainly ferrihydrite diffraction peaks. Moreover, the intensity of the few peaks due to the goethite phase decreased considerably in these latter samples. These measurements suggest the solubility limit of Cd in goethite is ~10 mol.%. Gerth (1990) reported a limit of 7.4 mol.%, though his conclusion was based on the results of a study that had only two samples having >5 mol.% Cd substitution. We observed some variation in the uptake of Cd, *i.e.* on occasions, not all the Cd present in the reaction mixture was incorporated into goethite (Table 1).

The synchrotron XRD patterns (Figure 1) were modelled using the computer program Rietica (Hunter, 1997) which utilizes the Rietveld method, a least-squares structural refinement technique in which the parameter of the structural model and of the instrumental conditions are optimized simultaneously (Rietveld, 1969). Two examples of fitted patterns are given in

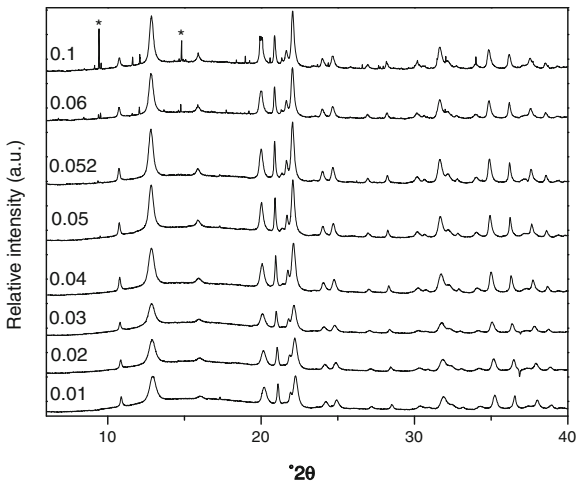

Figure 1. Synchrotron XRD patterns for Cd-substituted goethites, arranged in increasing values of x in $Fe_xCd_{1-x}OOH$. Two of the sharp peaks of Cd oxalate in the x = 0.1 sample are indicated by *. The broad feature near 15º is a consequence of the scattering from the capillary.

https://doi.org/10.1346/CCMN.2003.0510405 Published online by Cambridge University Press

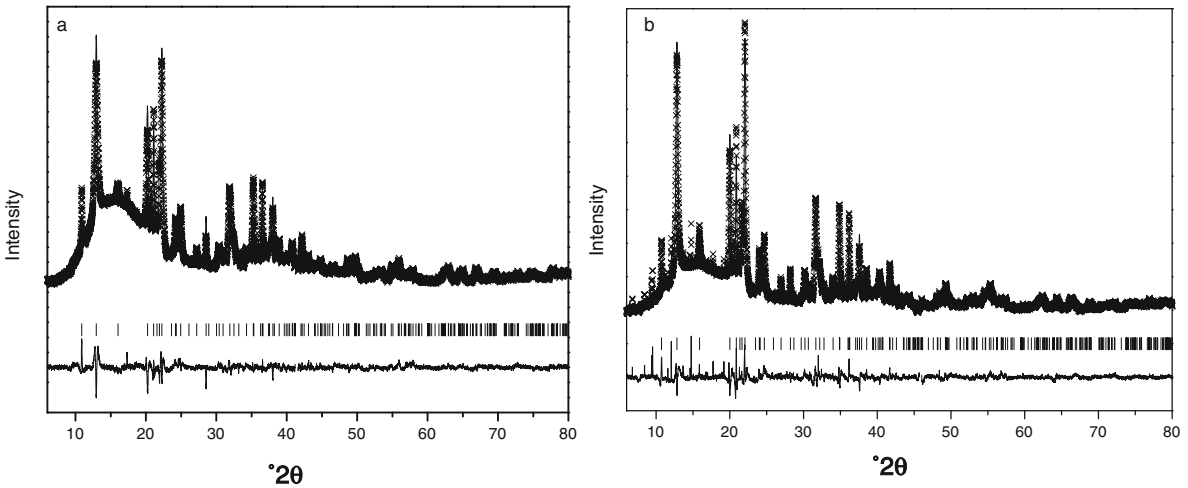

Figure 2. Observed (x), calculated, and difference profiles for synchrotron XRD profiles of Cd substituted goethites. (a) $x = 0.01$ in $Fe_xCd_{1-x}OOH$, Rp = 2.54%, Rwp = 3.12%, and GOF = 44.84, (b) $x = 0.06$ in $Fe_xCd_{1-x}OOH$, Rp = 1.68%, Rwp =1.912%, GOF = 35.77.

Figure 2. The $x = 0.01$ sample, in the series $Fe_{1-x}Cd_xOOH$, is a highly crystalline goethite sample which displays anisotropic broadening along the 0*kl* reflections. In the $x = 0.06$ and $x = 0.1$ samples additional peaks were observed, which were attributed to Cd oxalate. The Fe:Cd occupancy factors in the refinements were constrained so that the Fe:Cd ratio was that obtained from the chemical analysis (Table 1) and that the site was fully occupied. Also, the atomic positions and displacement parameters for the Fe and Cd were constrained to be equal.

Increasing Cd substitution resulted in a progressive increase in the cell volumes with each of the cell parameters increasing linearly (Table 2). This reflects the larger size of Cd^{2+} (0.95 Å) compared with Fe^{3+} (0.645 Å) (Shannon, 1976). The Fe–O (within octahedra) bond lengths did not vary between samples, whilst the Fe–OH (apical) bond lengths changed slightly with increasing Cd content, *i.e.* bond Fe–OH(1) shortened and bond Fe–OH(2) lengthened. The net result of these modifications on the average *M*–O distance was negligible (Figure 3).

The structural refinements indicate that the location of the cation is essentially unaltered by Cd substitution. Since the change in the average *M*–O distance upon incorporation of Cd is minimal there appears to be no structural reasons to limit the Cd content (Table 3). However, there are two constraints on substitution which were undetected by XRD. Firstly the replacement of Fe^{3+} with Cd^{2+} results in a charge imbalance which may be neutralized by the conversion of corner-sharing O^{2-} into OH^-. This may be expected to break down the goethite structure, which is built from the corner sharing network of dioctahedra (Figure 3). Secondly, as individual MO_6 octahedra enlarge, the hydrogen bonding across channels is weakened, reducing the net forces holding the goethite framework together. Therefore, the limit of Cd substitution may be attributed to a combination of the build up of negative charge, due to the replacement of Fe^{3+} with Cd^{2+}, or the weakening of covalent bonds and hydrogen bonding forces present in pure goethite (Deer *et al.*, 1980; Schulze, 1984; Schulze and Schwertmann, 1987).

Modifications to the cation-anion bonding were examined by FTIR. Peak broadening prevented identi-

Table 2. Unit-cell parameters of Cd-substituted goethites obtained from synchrotron XRD structural data. Values in parentheses are the estimated standard deviation for the last digit.

x in $Fe_{1-x}Cd_xOOH$	*a* (Å)	*b* (Å)	*c* (Å)	Unit-cell volume (Å^3)
0	4.6122(5)	9.9418(8)	3.0198(3)	138.43(3)
0.01	4.6148(4)	9.9427(5)	3.0189(2)	138.52(2)
0.02	4.6171(6)	9.9579(6)	3.0213(2)	138.91(3)
0.03	4.6277(5)	9.9820(6)	3.0283(2)	139.89(2)
0.04	4.6310(4)	10.0074(5)	3.0344(1)	140.63(2)
0.05	4.6323(1)	10.0221(4)	3.0365(1)	140.97(1)
0.052	4.6354(4)	10.0371(4)	3.0412(1)	141.50(2)
0.06	4.6393(5)	10.0514(6)	3.0447(2)	141.98(1)
0.10	4.6406(4)	10.0653(6)	3.0478(2)	142.36(2)

https://doi.org/10.1346/CCMN.2003.0510405 Published online by Cambridge University Press

Table 3. Fractional co-ordinates for samples $x = 0.01$ and $x = 0.1$, set in the *Pbnm* space group, used in the structural refinements.

	x	y	z	B^1 (Å^3)	Occupancy
$x = 0.01$					
Fe	0.0476(2)	0.8540(1)	0.25	0.15(6)	0.495
Cd	0.0476(2)	0.8540(1)	0.25	0.15(6)	0.005
O1	0.7170(10)	0.2046(4)	0.25	−0.26(10)	0.500
O2	0.2071(10)	0.0589(4)	0.25	0.08(11)	0.500
$x = 0.1$					
Fe	0.0464(3)	0.8550(1)	0.25	0.40(8)	0.451
Cd	0.0464(3)	0.8550(1)	0.25	0.40(8)	0.049
O1	0.7052(11)	0.2036(5)	0.25	-0.44(13)	0.500
O2	0.2049(14)	0.0549(5)	0.25	1.45(15)	0.500

[1]B is the isotropic atomic displacement parameter

fication of peak shifts to lower wavenumbers and this was expected since the electronic structure of Cd^{2+} ($4d^{10}$) leads to more covalent bonding than Fe^{3+} ($3d^5$) (Nakamoto, 1997).

A decrease in crystal size was observed in the TEM micrographs, which enabled direct measurements of the particle shape, size and orientation (Figure 4, Table 4). Lath-like crystals were present in each sample and both the breadth and length decreased in an approximately linear manner with increasing Cd content. The decrease in the length of goethite crystal was more rapid, 0.058 μm for each 1% increase in Cd^{2+}, than the breadth (~0.011 μm per 1% Cd). Schulze (1982) and Fey and Dixon (1981) found that crystal size in Al^{3+}-doped goethites decreases with increasing Al^{3+} content. Incorporation of Cd^{2+} in goethite structure possibly retards its crystal growth, which causes a decrease in both the length and breadth of the goethite crystals.

The TGA analysis of the various oxalate-treated samples showed a major weight loss of ~14 wt.% near 230ºC. The dehydroxylation temperature decreased regularly from 236ºC to 216ºC in the $x = 0.01$ to $x = 0.052$ series. In the $x = 0.06$ and $x = 0.1$ samples, the presence of oxalate groups broadened the dehydroxylation curves. The approximately linear decrease in the dehydroxylation temperature (236, 230, 228, 221, 218, 216ºC for the range of samples $x = 0.01$ to $x = 0.052$, respectively) is comparable to that observed in Mn^{3+}- and Ti^{4+}-substituted goethites (Wells, 1997). Substitution by Al^{3+} and Cr^{3+} increases the dehydroxylation temperatures (Schulze and Schwertmann, 1987). Wells (1997) suggested that this is a consequence of the larger M–O bond energies, *i.e.* Al–O (122.4 kcal/mol) and Cr–O (102.6 kcal/mol) bonds relative to that for Fe–O bonds (92.3 kcal/mol) (Lidi, 1999). By analogy, the lower Cd–O bond energy (56.3 kcal/mol) should decrease the dehydroxylation temperature, as is observed. Of course the stability of the samples will also be related to their crystallite size and morphology. In general, the smaller crystallites are expected to be more reactive and it can be proposed that the dehydroxylation temperature should decrease as the particle size decreases. Both features (*i.e.* bond strength and size) will contribute to the observed trend.

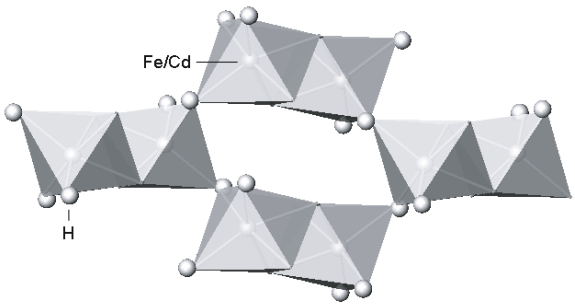

Figure 3. Representation of the goethite structure showing the 2×1 channels running down the c axis. The H atoms are represented by the small spheres, the Fe atoms are represented by the spheres enclosed in the octahedra.

There is only one site available for the Fe and Cd cations in the goethite structure, and the Fe and Cd will probably be randomly distributed within this site. Each of the two types of oxygen anions is bonded to three M cations and the statistical distribution of Fe and Cd will give rise to a range of M–O frequencies in the FTIR spectra. As the particle size decreases or the relative amount of surface hydroxyl groups, compared to the bulk, increases, the various FTIR features may also broaden. This was observed in the present study.

There is general agreement between the TEM and XRD studies with respect to both the morphology and size of the samples. It appears that the needles observed in the TEM studies are single crystals. Clearly the incorporation of Cd into the goethite structure inhibits crystal growth, though the development along any individual crystalline face does not appear to be affected. The ratio of the length:breadth of the samples observed in the TEM is remarkably constant (Table 4).

https://doi.org/10.1346/CCMN.2003.0510405 Published online by Cambridge University Press

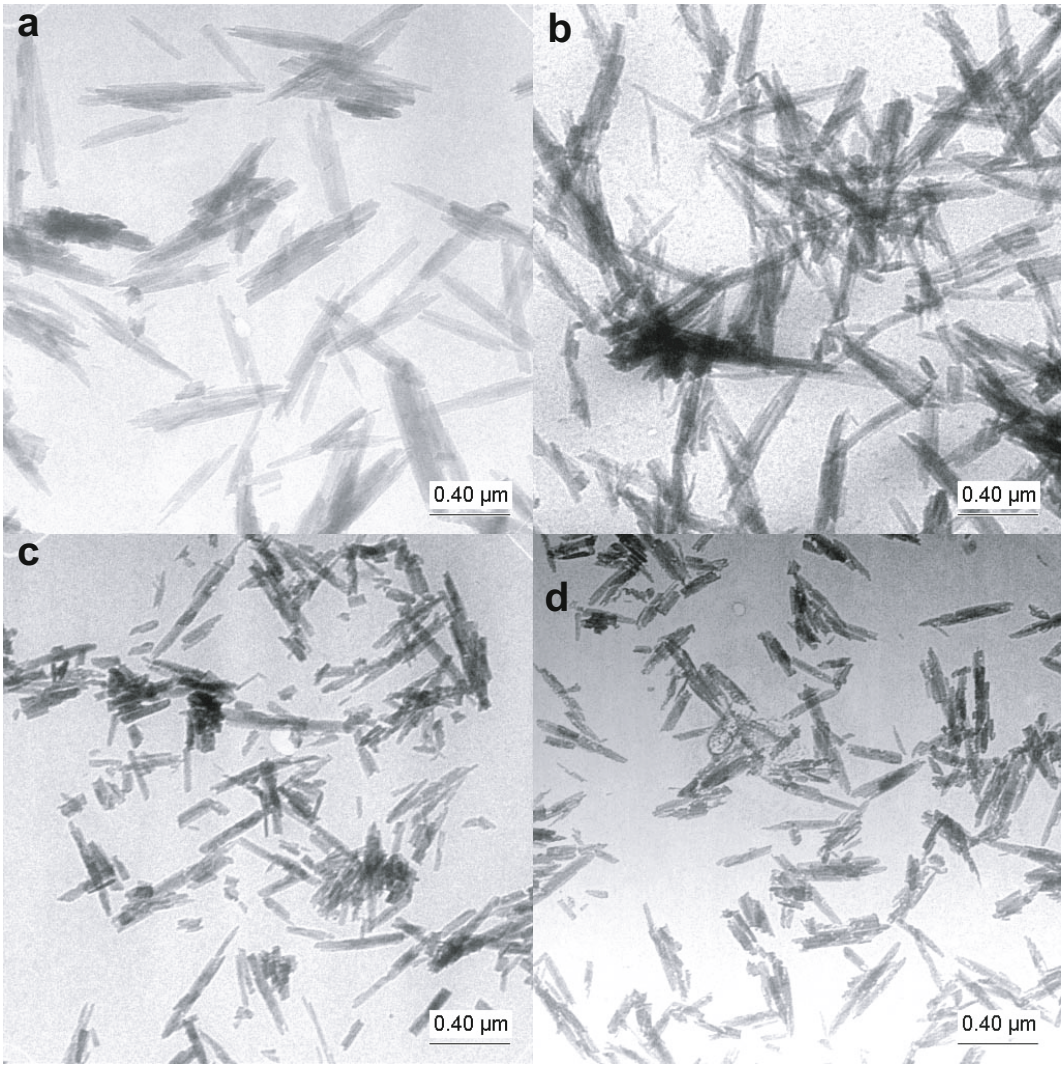

Figure 4. TEM images of Cd-substituted goethites. (a) $x = 0.01$ in $Fe_xCd_{1-x}OOH$, (b) $x = 0.02$ in $Fe_xCd_{1-x}OOH$, (c) $x = 0.052$ in $Fe_xCd_{1-x}OOH$, (d) $x = 0.1$ in $Fe_xCd_{1-x}OOH$.

Table 4. Mean, median and standard error (SE) values for breadth, length and area, and the mean breadth/length for Cd-substituted goethite crystals derived from TEM images.

Samples	n*	Breadth (μm)			Length (μm)			Area (μm^2)			Length/
x		Mean	Median	SE	Mean	Median	SE	Mean	Median	SE	breadth
0	56	0.184	0.171	0.008	0.843	0.841	0.032	0.070	0.059	0.007	4.6
0.01	55	0.139	0.137	0.005	0.680	0.612	0.031	0.056	0.055	0.005	4.4
0.02	86	0.129	0.128	0.004	0.640	0.609	0.024	0.050	0.045	0.003	4.7
0.03	55	0.103	0.101	0.003	0.567	0.551	0.028	0.039	0.035	0.003	5.3
0.04	15	0.075	0.068	0.008	0.396	0.324	0.055	0.020	0.013	0.004	4.3
0.05	50	0.136	0.125	0.008	0.612	0.596	0.056	0.059	0.052	0.005	4.3
0.052	76	0.079	0.075	0.003	0.343	0.336	0.014	0.019	0.017	0.001	4.3
0.06	81	0.081	0.077	0.004	0.387	0.336	0.024	0.024	0.018	0.003	4.1
0.1	78	0.067	0.061	0.002	0.264	0.252	0.011	0.013	0.010	0.001	3.8

* Number of crystals measured to derive various morphological parameters. The crystal area was calculated by summing all of the contiguous pixels in the image.

https://doi.org/10.1346/CCMN.2003.0510405 Published online by Cambridge University Press

CONCLUSIONS

Cadmium can be incorporated by isomorphous substitution of up to ~9.5% of the Fe^{3+} ions in the octahedra of goethite. The limit of substitution was attributed to both the build up of negative charge, due to the replacement of Fe^{3+} with Cd^{2+}, and the weakening of covalent bonds and hydrogen bonding forces present in pure goethite. Analysis by synchrotron XRD and TEM indicated that incorporation of Cd led to increases in all unit-cell parameters but an overall decrease in crystallite size. Further work is required to investigate the local structure of the Cd cations, by XANES and EXAFS analyses.

ACKNOWLEDGMENTS

The measurements performed at the Australian National Beamline Facility were supported by the Australian Synchrotron Research Program, which is funded by the Commonwealth of Australia under the Major National Research Facilities. An international scholarship was provided by AusAID to assist T. Huynh in her research at the University of Sydney. This work was partially supported by a Sesquicentenary Grant from The University of Sydney.

REFERENCES

Cornell, R.M. and Giovanoli, R. (1988) The influence of copper on the transformation of ferrihydrite ($5Fe_2O_3.9H_2O$) into crystalline products in alkaline media. *Polyhedron*, **7**, 385–391.

Cornell, R.M. and Schwertmann, U. (1996) *The Iron Oxides*. VCH, Weinheim, Germany.

Deer, W.A., Howie, R.A. and Zussman, J. (1980) *An Introduction to the Rock Forming Minerals*. Longmans, London.

Fey, M.V. and Dixon, J.B. (1981) Synthesis and properties of poorly crystalline hydrated aluminous goethites. *Clays and Clay Minerals*, **29**, 91–100.

Gerth, J. (1990) Unit-cell dimensions of pure and trace metal-associated goethites. *Geochimica et Cosmochimica Acta*, **54**, 363–371.

Hunter, B.A. (1997) *Rietica for Windows 1.74*. ANSTO, Sydney, Australia.

Lidi, D. (1999) *CRC Handbook of Chemistry and Physics 1998–1999*. CRC, Boca Raton, Florida.

Lim-Nunez, R. and Gilkes, R.J. (1987) Acid dissolution of synthetic metal-containing goethites and hematites. Pp. 197–204 in: *Proceedings of the International Clay Conference Denver, 1985* (L.G. Schultz, H. van Olphen and F.A. Mumpton, editors). Clay Minerals Society, Bloomington, Indiana.

Nakamoto, K. (1997) *Infrared and Raman Spectra of Inorganic and Coordination Compounds, Part A: Theory and Applications in Inorganic Chemistry*. John Wiley & Sons, New York.

Rietveld, H.M. (1969) A profile refinement method for nuclear and magnetic structures. *Journal of Applied Crystallography*, **2**, 65–71.

Schulze, D.G. (1982) The identification of iron oxides by differential X-ray diffraction and the influence of aluminium substitution on the structure of goethite. PhD thesis, Technical University of München, Freising-Weihenstephan, Germany.

Schulze, D.G. (1984) The influence of aluminum on iron oxides, VIII. Unit cell dimensions of Al-substituted goethites and estimation of Al from them. *Clays and Clay Minerals*, **32**, 36–44.

Schulze, D.G. and Schwertmann, U. (1987) The influence of aluminium on iron oxides: XIII. Properties of goethites synthesized in 0.3 M KOH at 25 ºC. *Clay Minerals*, **22**, 83–92.

Schwertmann U. (1964) Differenzierung der Eisenoxide des Bodens durch Extraktion mit Ammoniumoxalat-Lösung. *Zeitschrift für Pflanzenernährung Düngung und Bodenkunde*, **105**, 194–202.

Schwertmann, U. and Carlson, L. (1994) Aluminum influence on iron oxides: XVII. Unit-cell parameters and aluminum substitution of natural goethites. *Soil Science Society of America Journal*, **58**, 256–261.

Schwertmann, U., Gasser, U. and Sticher, H. (1989) Chromium for iron substitution in synthetic goethites. *Geochimica et Cosmochimica Acta*, **53**, 1293–1297.

Shannon, R.D. (1976) Revised effective ionic radii and systematic studies of interatomic distances in halides and chalcogenides. *Acta Crystallographica*, **A32**, 751–767.

Singh, B. (2001) Heavy metals in soils: sources, chemical reactions and forms. Pp. 77–93 in: *Environmental Geotechnics* (D. Smith, S. Fityus and M. Allman, editors). Proceedings of the 2nd Australia and New Zealand Conference on Environmental Geotechnics-Geoenvironment 2001. Australian Geomechanical Society, Newcastle, Australia.

Singh, B. and Gilkes, R.J. (1992) Properties and distribution of iron oxides and their association with minor elements in the soils of South-western Australia. *Journal of Soil Science*, **43**, 77–98.

Wells, M.A. (1997) Mineral, chemical and magnetic properties of synthetic, metal-substituted goethite and hematite. PhD thesis, University of Western Australia, Perth, Australia.

(*Received 15 November 2002; revised 19 March 2003; Ms. 739*)